Journal of Catalysis 270 (2010) 110–124

Contents lists available at ScienceDirect

Journal of Catalysis

journal homepage: www.elsevier.com/locate/jcat

Catalytic fast pyrolysis of glucose with HZSM-5: The combined homogeneous and heterogeneous reactions

Torren R. Carlson [a], Jungho Jae [a], Yu-Chuan Lin [b], Geoffrey A. Tompsett [a], George W. Huber [a,*]

[a] Department of Chemical Engineering, 159 Goessmann Laboratory, University of Massachusetts, Amherst, MA 01003, USA
[b] Department of Chemical Engineering & Materials Science, Yuan Ze University, Chungli 32003, Taiwan

ARTICLE INFO

Article history:
Received 6 September 2009
Revised 9 December 2009
Accepted 13 December 2009
Available online 4 February 2010

Keywords:
Catalyst
Pyrolysis
Glucose
ZSM-5
Mechanism

ABSTRACT

The production of aromatics from glucose by catalytic fast pyrolysis occurs in two steps. First, glucose is thermally decomposed to smaller oxygenates through retro-aldol fragmentation, Grob fragmentation and dehydration reactions. At low temperatures (<300 °C), retro-aldol and Grob fragmentation reactions are favored with D-glyceraldehyde, hydroxyacetone and hydroxyacetaldehyde being the primary products. At higher temperatures (>300 °C), dehydration is favored with levoglucosan as the major product. The addition of ZSM-5 catalyst to the pyrolysis reactor lowers the temperature at which the fragmentation and dehydration reactions occur at 206 °C and 312 °C, and at 282 °C and 369 °C, respectively. In the second step of catalytic fast pyrolysis, the dehydrated products enter into the catalyst where they are converted into aromatics, CO, CO_2 and water. The catalytic conversion step is significantly slower than the initial pyrolysis reaction. The aromatic product selectivity is a function of catalyst to glucose weight ratio, heating rate and reaction temperature. At 600 °C, a maximum carbon yield of 32% aromatics is realized after 240 s with catalysts to feed ratio of 19. The major competing reaction to aromatic production is the formation of coke. Coke is most likely formed by polymerization of the furans on the external catalyst surface.

1. Introduction

Lignocellulosic biomass is being studied worldwide as a feedstock for renewable liquid biofuels due to its low cost and abundance [1–4]. Lignocellulosic biomass is not currently used as a liquid fuel feedstock because the economical processes for its conversion has yet to be developed [1]. Catalytic fast pyrolysis (CFP) is a promising method for the direct conversion of solid biomass into gasoline range aromatic products [5–12]. CFP involves the pyrolysis of biomass in the presence of zeolites. In the first step of this reaction, the solid biomass is rapidly heated (>500 °C s^{-1}) to intermediate temperatures (400–600 °C). The importance of pyrolysis heating rate is well known [13,14]. At these high temperatures, the biomass readily decomposes into pyrolysis vapors. These pyrolysis vapors then enter into the zeolite catalyst pores where they are converted into aromatics, CO, CO_2 and H_2O. One advantage of CFP is that solid biomass is directly converted into liquid aromatic fuel in a single reactor with short residence times. Hence, conversion is rapid, continuous and uncomplicated. Thus, all the reaction chemistry occurs in one single reactor, which is advantageous compared to gasification and fermentation technologies which all require a number of different reactors.

Several researchers have used zeolite catalysts for conversion of biomass-derived feedstocks into aromatics. This includes the early work in the 1980s by Chen et al. [15] and Haniff and Dao [16,17] on the conversion of carbohydrate feeds. Chen et al. [15] reported that aqueous glucose solutions can be converted to hydrocarbons in a fixed bed reactor operated at 510 °C. Hanniff and Dao [17] also reported that glucose could be converted in a microreactor with ZSM-5 as well as Mn-ZSM-5 and Zn-ZSM-5. However, they reported low yields of hydrocarbons as polymerization of the carbohydrate feed was favored at temperatures above 350 °C. In addition to direct conversion of carbohydrates, several researches have studied the upgrading of pyrolysis oils with zeolite catalysts [18–23]. Horne and Williams [22] reported a threefold increase in aromatic yield when the pyrolysis vapors from a fluidized bed reactor were passed over a secondary fixed bed of ZSM-5 catalyst.

More recently, high aromatic yields have been obtained from lignocellulosic biomass in one step by introducing zeolite catalysts directly into various types of pyrolysis reactors [5,7,8,11,12]. We have recently reported that for wood and cellulose pyrolysis with ZSM-5 in a fixed bed microreactor, about 35% to 50% of the theoretical yield for aromatics can be obtained from wood and cellulose feeds, respectively [5]. Pattiya et al. [11] used a similar fixed bed microreactor to study the catalytic pyrolysis of cassava rhizome. Out of the four catalysts tested, ZSM-5, Al-MCM-41 and Al-MSU-F and a proprietary alumina-stabilized ceria

* Corresponding author. Fax: +1 413 545 1647.
E-mail address: huber@ecs.umass.edu (G.W. Huber).

0021-9517/$ - see front matter © 2010 Elsevier Inc. All rights reserved.
doi:10.1016/j.jcat.2009.12.013

MI-575, ZSM-5 yielded the highest amount of aromatics in the resulting bio-oil.

Several researchers have also performed catalytic pyrolysis in continuous fluidized bed reactors [7,8,12]. Olazar and coworkers [8] reported high yields of aromatics (28% of the theoretical yield) in a canonical spouted bed reactor using ZSM-5 catalyst. Aho et al. [12] tested several types of zeolites for the catalytic pyrolysis of softwood in a fluidized bed reactor. They reported that β-zeolite, mordenite, Y-zeolite and ZSM-5 all produced different product spectra in the resulting bio-oil. The addition of ZSM-5 significantly decreased the amount of acids and alcohols in the bio-oil, while the amount of ketones was increased. Lappas and collaborators [7] reported on the use of a laboratory-scale FCC unit for the catalytic pyrolysis of pine wood with a commercial fluid catalytic cracking catalyst and a commercial ZSM-5 additive. They reported that addition of catalyst increased the yield of water, non-condensable gases and char. The bio-oil obtained was of lower oxygen content and therefore of better quality.

The mechanism of catalytic conversion of biomass to aromatics over a zeolite catalyst is not fully understood, however, there is evidence of many of the general reaction steps. CFP involves the homogeneous thermal decomposition of the biomass to smaller oxygenates [24–26]. These oxygenates are then dehydrated. The dehydrated oxygenates diffuse into the zeolite catalyst pores where they undergo a series of oligomerization, decarbonylation and dehydration reactions to produce aromatics, CO, CO_2 and water at the active sites [27]. Isotopic studies of CFP for ^{13}C and ^{12}C glucose have shown that the oxygenates are all monoistopic and the aromatics produced are a random mixture of ^{13}C and ^{12}C [27]. This indicates that the aromatics are produced from a hydrocarbon pool composed of the decomposed oxygenated compounds. The major challenge with CFP is to avoid undesired coke formation, which can be produced from both homogeneous and heterogeneous reactions [6]. The purpose of this paper is to study the combined homogeneous and heterogeneous reactions that occur during CFP of glucose on ZSM-5.

Lignocellulosic biomass is a complex natural material composed of three components: cellulose, hemicellulose and lignin [28]. During pyrolysis, mono and oligosaccharides are the primary thermal decomposition products from cellulose and hemicellulose [29,30]. Furthermore, we have recently shown similar aromatic yields and product selectivity are obtained for CFP of both glucose and cellulose [5,6]. For these reasons, and in order to simplify the analysis, glucose is chosen as a model compound to study the reactions involved during CFP.

In this paper, we will propose the overall reaction pathway for the conversion of glucose to aromatics by CFP. The initial thermal decomposition of pure glucose and glucose in the presence of ZSM-5 will be studied with TG/DTG, ex situ FTIR and visual observation. Ex situ FTIR will also be used to determine which species are involved in the undesired coke formation reactions. Furthermore, nitrogen adsorption will be used to determine whether these undesired reactions occur on the surface or within the pores of the catalyst. A pyroprobe reactor coupled to a GC/MS will primarily be used to study how yield and selectivity for aromatics changes with different reaction conditions as well as to study the conversion of reaction intermediates.

2. Experimental

2.1. Pyroprobe

Fast pyrolysis experiments were conducted using a model 2000 pyroprobe analytical pyrolizer (CDS Analytical Inc.). The probe is a computer-controlled resistively heated element that holds an open-ended quartz tube (pictured in Fig. 1). Powdered samples are held in the tube with loose quartz wool packing; during pyrolysis, vapors flow from the open ends of the quartz tube into a larger cavity (the pyrolysis interface) with a helium carrier gas stream.

The carrier gas stream is routed to a model 5890 gas chromatograph (GC) interfaced with a Hewlett Packard model 5972A mass spectrometer (MS). The pyrolysis interface was held at 100 °C, and the GC injector temperature used was 275 °C. Helium was used as the inert pyrolysis gas as well as the carrier gas for the GC/MS system. A 0.5 ml min^{-1} constant flow program was used for the GC capillary column (Restek Rtx-5sil MS). The GC oven was programmed with the following temperature regime: hold at 50 °C for 1 min, ramp to 200 °C at 10 °C min^{-1}, hold at 200 °C for 15 min. Products were quantified by injecting calibration standards into the GC/MS system. All yields are reported in terms of molar carbon yield where the moles of carbon in the product are divided by the moles of carbon in the reactant. The aromatic selectivity reported is defined as the moles of carbon in an aromatic species divided by the total moles of aromatic species carbon. Similarly, the oxygenate selectivity is defined as the moles of carbon in an oxygenated species divided by the total moles of oxygenated species carbon.

Bulk powdered reactants were prepared by physically mixing the glucose feed and the catalyst. For a typical run, between 8 and 15 mg of bulk reactant–catalyst mixture was added to the reactor. Both the feed and the catalyst were sieved to less than 140 mesh before mixing. The physical mixtures of glucose were prepared with a ZSM-5 (Si/Al = 15, WR Grace) to D-glucose (Fisher) ratio of 19, 9, 4, 2.3 and 1.5.

For the speciation and quantification of pure glucose pyrolysis products (which are mostly thermally unstable), an in-house-designed trap was employed. The trap consists of a 25 mL Pyrex vial, a screw-tight frame with plug-valve-controlled gas inlet and outlet, and the pyroprobe pyrolizer. A ¼-in. channel allows the pyroprobe pyrolizer to be inserted from the top of frame into the center of vial. Prior to each trial, the vial was flushed with ultra-high purity helium at 50 mL min^{-1} flow rate for 10 min. After purging, the vial is made gastight by closing the outlet and inlet valves. The trap is then transferred in a dewar flask with a liquid nitrogen bath at −196 °C, which allows rapid quenching of volatiles evolved during reaction. After reaction, the condensed products on the walls of the vial are quantitatively removed with 1 mL of methanol. The methanol solution is then analyzed using a GC–MS (Shimadzu GC-2010 and QP2010S, analytes separated by Restek RTX-VMS).

2.2. Thermogravimetric analysis with mass spectrometry (TGA-MS)

Thermogravimetric analysis was performed with a Q600 TGA system (TA Instruments). A quadruple mass spectrometer (Extorr XT 300) was coupled via a heated line to the TGA to measure the volatile species produced during pyrolysis. The heated transfer line was held at 250 °C to circumvent condensation of the product vapors. A low electron ionization voltage of 29 eV was used to suppress secondary fragmentation. The total pressure of ion source was 10^{-6} Torr. The ions measured for each run include 2, 16, 18, 28, 44, 78, 91 and 128 *m/z*. Ultra-high-purity helium (Airgas, NH) was used as the sweeper gas with a flow rate of 100 mL min^{-1}. External and internal mass transfer limitations were investigated by varying sweeper gas flow rates (from 50 to 200 mL min^{-1}) and particle sizes (from 40 to 325 mesh). Both of them were found to be negligible. For a typical run, approximately 5 mg of powdered sample was used for pure glucose pyrolysis and about 30 mg for the glucose–ZSM-5 mixture. Prior to all trials, samples were preheated to 110 °C for 30 min, under helium flow, to remove physically adsorbed water. Pyrolysis was then carried out from 50 °C to 600 °C with a designated heating rate (0.017, 0.25 or 2.5 °C s^{-1}).

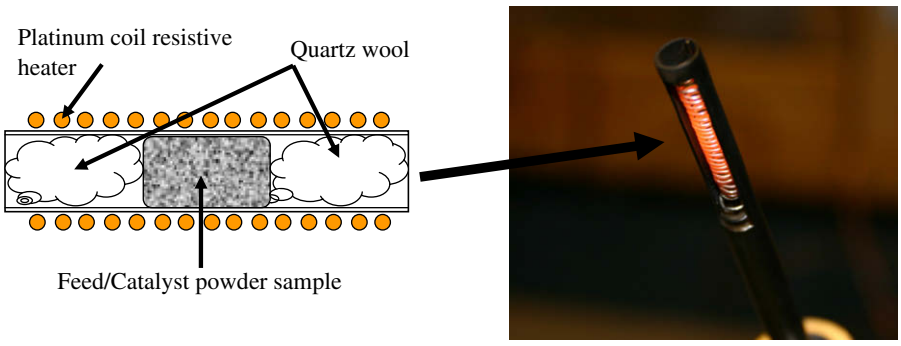

Fig. 1. Diagram of the pyroprobe reactor setup. On the left, a schematic cross-section of the prepared sample is pictured (not to scale). Powdered reactants and catalysts are held with loose quartz wool packing. Pictured on the right is the resistively heated element, which holds the sample tube (2 mm × 25 mm). During reaction, product vapors flow from the open ends of the sample tube into the GC/MS interface via a helium sweeper gas stream.

2.3. Fourier-transform infrared (FTIR)

FTIR spectra were obtained from the zeolite samples using a Bruker Equinox 55 infrared spectrometer. The KBr method was employed using spectroscopic grade KBr mixed with the zeolite/glucose in a 100:5 weight ratio. An average of 50 scans at 4 cm^{-1} resolution was obtained for each KBr pellet. This method is as used by Bilba and Ouensanga [31] and Sharma and coworkers [32]. KBr pellet method was used due to the low quantity of samples prepared using the pyroprobe reactor.

2.4. Elemental analysis (EA)

Carbon on the spent catalyst was quantified by elemental analysis (performed by Schwarzkopf Microanalytical Laboratory, NY). The missing carbon can be attributed to the non-quantified thermally unstable oxygenated species (which cannot be detected in our experimental setup) and coking of the pyrolysis interface or transfer lines.

2.5. Catalyst

ZSM-5 zeolite used for these experiments was a commercial zeolite catalyst from WR Grace, with a silicon to aluminum ratio equal to 15. This catalyst was calcined at 550 °C in air for 5 h prior to the pyrolysis experiments. The catalyst and mixtures of ZSM-5/glucose were stored in sealed vials in a desiccator in order to minimize the adsorption of atmospheric moisture.

2.6. Nitrogen adsorption

Nitrogen adsorption experiments were carried out at the normal boiling point of N_2 (−196 °C) for the determination of micropore volume (t-method) using an AUTOSORB®-1-MPC (Quantachrome Instruments; Boynton Beach, FL) gas adsorption system. Prior to the measurement, the samples were outgassed at 300 °C for 24 h under vacuum. Coked catalyst samples were prepared by using the catalyst after reaction at 600 °C for 240 s, mixing fresh glucose at 5 wt.% and 30 wt.% and running a samples pyrolysis treatment at 600 °C for 240 s.

3. Results

3.1. Thermal decomposition of glucose

3.1.1. Pyroprobe results

Fig. 2 shows the detailed quantification of glucose pyrolysis with 1000, 2.5 and 0.25 °C s^{-1} heating rates carried out with the in-house-designed trap. The dehydration product, levoglucosan (LGA, 1,6-anhydro-β-D-glucopyranose, $C_6H_{10}O_5$), was found to be the most abundant product. Other anhydrosugars such as levoglucosenone (LGO, 6,8-dioxabicyclo[3.2.1]oct-2-en-4-one, $C_6H_6O_3$), 1,4:3,6-dianhydro-β-D-glucopyranose (DGP, $C_6H_8O_4$) and 1,6-anhydro-β-D-glucofuranose (AGF, $C_6H_{10}O_5$) were present in lower amounts. Products that are likely formed from the retro-aldol condensation of glucose such as D-glyceraldehyde, hydroxyacetone and hydroxyacetaldehyde were also observed. The selectivity for coke ranges from 30% to 40% carbon. As the heating rate increases, the LGA yield increases, while the coke yield decreases. A lower heating rate increases the amount of dehydration reactions, with greater DGP, LGO and coke.

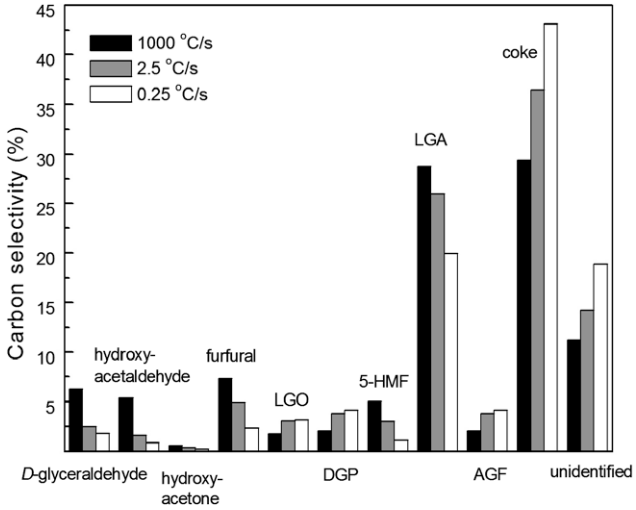

Fig. 2. Product distribution for glucose pyrolysis with 1000, 2.5 and 0.25 °C s^{-1} heating rates from pyroprobe reactor with liquid N_2 trap. Final temperature at 600 °C with reaction time for 240 s.

3.1.2. Themogravimetric analysis with mass spectrometry (TGA-MS)

Table 1 summarizes the approximate and elemental analysis of glucose pyrolysis products after a 2.5 °C s^{-1} heating rate. Around 89 wt.% of glucose can be volatilized, with 11% of fixed carbon and trace ash. Water, CO and CO_2 are the major species identified by the TGA-MS. The CO and CO_2 are formed from degradation of the primary pyrolysis products (e.g. levoglucosan, hydroxyacetaldehyde), which occurs in the line leading from the TGA to the MS. Only small amounts of these primary pyrolysis products are observed in our TGA-MS system. These primary pyrolysis products

Table 1
Proximate and elemental analysis of glucose pyrolysis.

Proximate analysis (wt.%)			Elemental analysis (wt.%)		
Volatile	Fixed C.	Ash	C	H	O[a]
89.0	10.9	0.1	42.9	6.5	50.6

[a] By balance.

can only be observed if they are quickly condensed out, as with the liquid nitrogen trap in Section 3.1.1.

Fig. 3a and b shows the DTG and MS signals of pure glucose pyrolysis with 0.017, 0.25 and 2.5 °C s^{-1} heating rates. Glucose pyrolysis initiates at 150, 200 and 250 °C, respectively. The DTG curves of all pyrolysis rates are composed of two major peaks. For a heating rate of 0.017 °C s^{-1}, the peaks are located at 198 and 290 °C, with almost equivalent intensity of the two peaks. For 0.25 °C s^{-1}, the first peak is at 228 °C; the second, 312 °C. For 2.5 °C s^{-1}, the first peak is at 282 °C; the second, 369 °C. The intensity of the first DTG peak diminishes as the heating rate is increased. Fig. 3b shows the corresponded MS responses at a 2.5 °C s^{-1} heating rate. The ion fragments, including hydrogen (m/z = 2), methane (m/z = 16), water (m/z = 18), carbon monoxide/ethylene (m/z = 28) and carbon dioxide (m/z = 44), were recorded with time. From the 28 m/z and 44 m/z signals, it is seen that decarboxylation and water removal begins around 200 °C, while decarbonylation, methane production and hydrogen production do not initiate until above 250 °C. Water is removed during two separate reactions, the first taking place at ~300 °C and the second at ~410 °C. The water MS signal corresponds to the two separate DTG peaks indicating both of these reactions involve the removal of water. In Fig. 3c, the DTG curves for the pyrolysis of glucose with ZSM-5 (19:1 catalyst to glucose wt. ratio) are shown. The DTG responses for different heating rates show similar peaks to the non-catalyzed pyrolysis, however, the two peaks shift to lower temperature. For the heating rates of 0.017, 0.25 and 2.5 °C s^{-1}, the first DTG peak shifts to 154, 171 and 206 °C, respectively. The second DTG peaks also shift downward to 275, 282 and 312 °C for the 0.017, 0.25 and 2.5 °C s^{-1} heating rates, respectively. When glucose was pyrolyzed in the presence of ZSM-5, a third peak appears. This new peak is located at 327, 363 and 402 °C for the 0.017, 0.25 and 2.5 °C s^{-1} heating rates, respectively. In Fig. 3d, the MS responses for the pyrolysis of glucose with ZSM-5 at a heating rate of 2.5 °C s^{-1} are shown. Compared to pure glucose pyrolysis, the MS signals initiate at a lower temperature (m/z = 28 at 50 °C; m/z = 18 at 100 °C). At around 350 °C, where the newly formed third DTG peak is located, m/z = 78 (benzene) and m/z = 91 (toluene) signals are observed. The response of m/z = 28 shows a second peak around the same temperature. The second m/z = 28 peak is most likely from ethylene. It is well documented in the literature for the methanol to hydrocarbons process with ZSM-5 catalyst that ethylene is formed concurrently with benzene and toluene [33]. Comparing both trials, almost all the MS ions in Fig. 3d show significant higher responses and greater areas under the MS peaks than those in Fig. 3b, except m/z = 16 (methane). This is because for pyrolysis without catalyst, the major products are oxygenates that are not shown in the MS response. For pyrolysis with catalyst, the oxygenates are converted to water, CO, CO_2 and aromatics. These product ions are shown in the MS response, which leads to an increase in the total ions measured.

The two separate peaks in the DTG response for glucose pyrolysis imply two separate decomposition reactions. To identify the species that are present for each peak, separate pyrolysis runs were carried out using identical reaction conditions, however, the temperature ramp was stopped at the onset of the peak of interest. At this designated temperature, the reaction was rapidly quenched by cooling the furnace to room temperature with cooling air. The quenched reaction residue was then quantitatively dissolved in methanol and analyzed by GC/MS. For low-temperature products, the final temperatures and their corresponding heating rates were

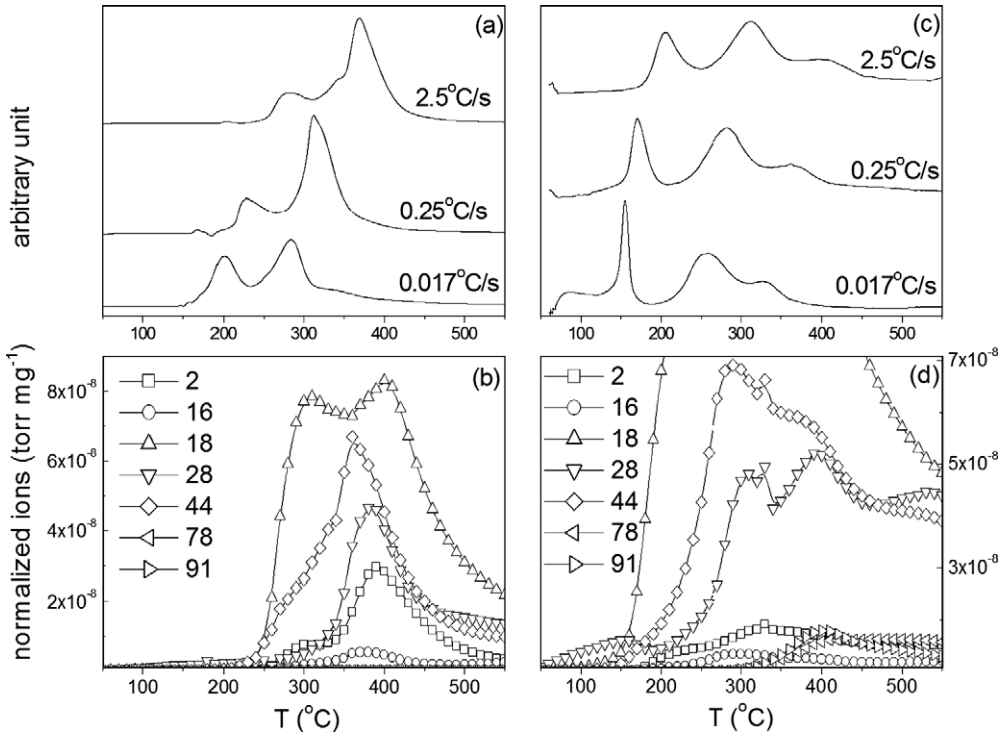

Fig. 3. (a) DTG signals of glucose pyrolysis; (b) MS responses of selected ions of glucose pyrolysis at a 2.5 °C s^{-1} heating rate; (c) DTG signals of glucose pyrolysis with ZSM-5; (d) MS responses of selected ions of glucose pyrolysis with ZSM-5 at a 2.5 °C s^{-1} heating rate.

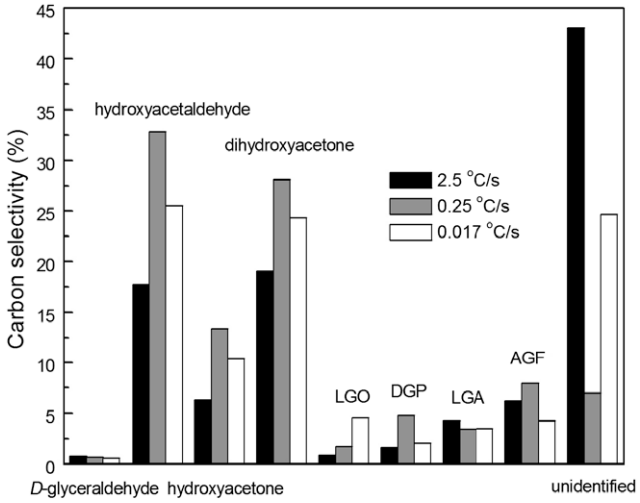

Fig. 4. Carbon yields of glucose pyrolysis with three pyrolysis rates, final temperatures at 180 (0.017 °C s^{-1}), 200 (0.25 °C s^{-1}) and 250 °C (2.5 °C s^{-1}), respectively.

180 °C for 0.017 °C s^{-1}, 200 °C for 0.25 °C s^{-1} and 250 °C for 2.5 °C s^{-1}. At these temperatures, the residues of all samples are ~98% of the initial sample mass. Fig. 4 shows the distribution of the species within the methanol-dissolved residue for the three different heating rates. The primary products observed for the low-temperature peak were hydroxyacetaldehyde, hydroxyacetone and dihydroxyacetone. These products are likely from retro-aldol and Grob fragmentation of glucose [25,26]. As shown in Fig. 4, the unidentified carbon is quite high for the lowest heating rate (2.5 °C s^{-1}). This missing carbon could be attributed to other reactions other than retro-aldol and Grob fragmentation. For the high-temperature peak, the final temperatures were 280, 300 and 380 °C for the 0.017, 0.25 and 2.5 °C s^{-1} heating rate runs, respectively. At these temperatures, only non-dissolvable coke remained in the crucible.

3.1.3. Visual observations

To provide a clear view of glucose fast pyrolysis and catalytic fast pyrolysis, a series of snapshots of these experiments are shown in Fig. 5. Both trials were carried out in the Pyrex trap with a 1000 °C s^{-1} heating rate and final temperature at 600 °C. Instead of immersing collectors into the liquid nitrogen dewar, the Pyrex vial was set on the bench top and filmed with a video camera at room temperature. Fig. 5 shows the solid pure glucose (a) and glucose–ZSM-5 mixture (e) at room temperature before reaction. Fig. 5b and f shows snapshots at ~210 °C during pyrolysis of the glucose and glucose–ZSM-5 mixture, respectively. At 210 °C, glucose transforms into a transparent liquid phase because such a pyrolysis temperature surpasses the boiling point (~145 °C) [34]. As seen in Fig. 5f, at 210 °C, black spots (coke) are clearly visible. At this same temperature, no coke is observed when the catalyst is not present during pyrolysis. This indicates that coke forms at a lower temperature when catalysts are present. At a temperature of 600 °C (Fig. 5c and g), vapors can be seen coming from the ends of the quartz tube. At 600 °C, the coke formation becomes more severe for the glucose/ZSM-5 sample (Fig. 5g). After 5 s at the final temperature, the residual of glucose inside the reactor turns into coke for both cases in (Fig. 5d and h).

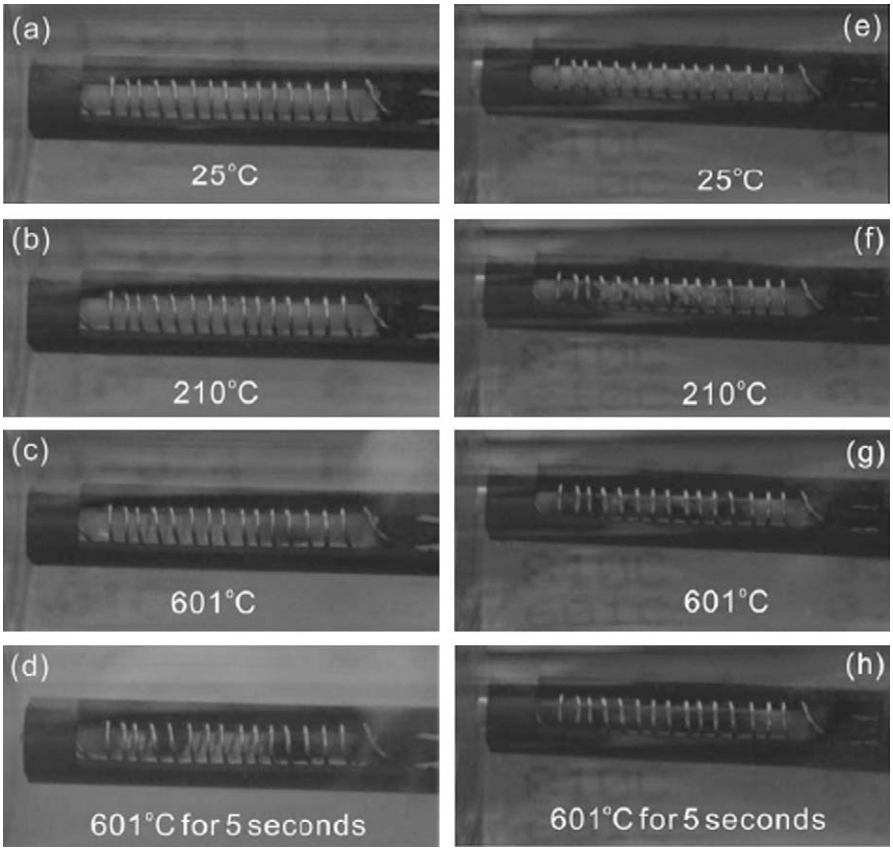

Fig. 5. Comparison of glucose fast pyrolysis (a–d) and glucose/ZSM-5 pyrolysis (e–h; glucose-to-ZSM-5 = 1:19).

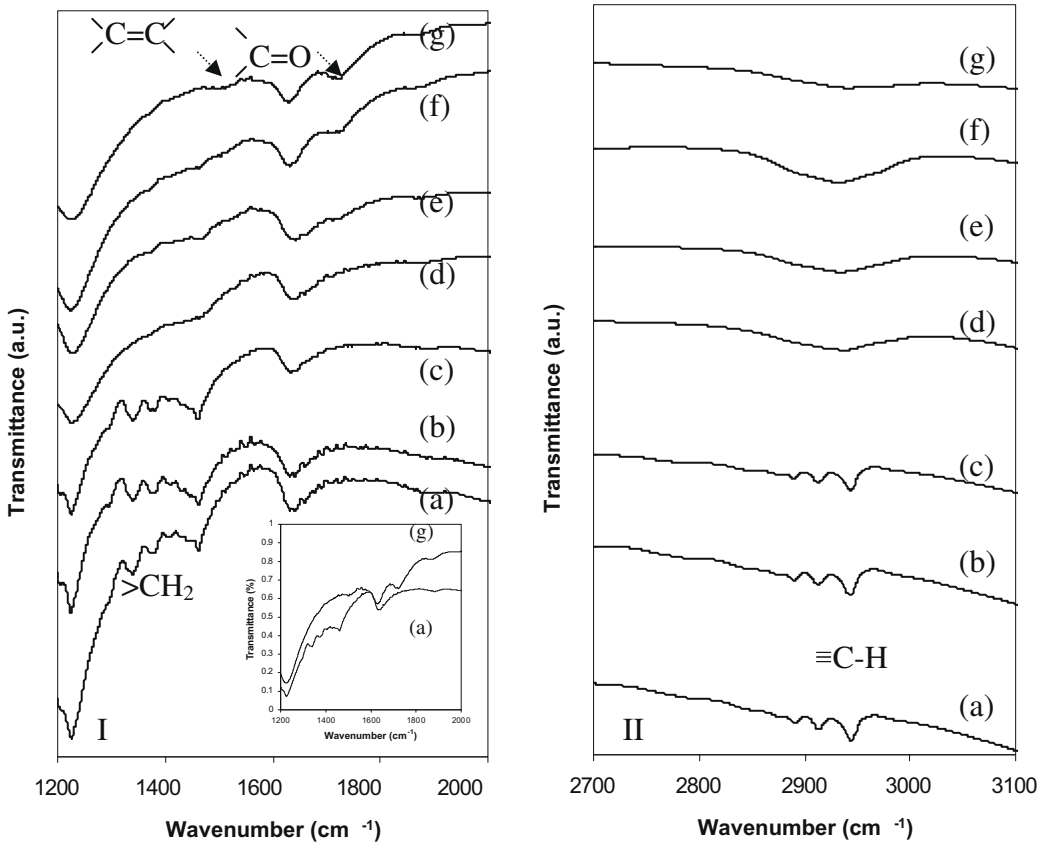

Fig. 6. IR spectra for glucose pyrolysis in the presence of ZSM-5 (catalyst to feed ratio = 1.5) at 100 °C s^{-1} to a final temperature of: (a) unreacted (b) 100 °C, (c) 200 °C, (d) 300 °C, (e) 400 °C, (f) 500 °C (g) and 600 °C. (I) 1200–2000 cm^{-1} region and (II) 2700–3100 cm^{-1} region. Spectra are off-set to show the bands.

Table 2
Infrared band positions (cm^{-1}) and assignments for the fast pyrolysis of glucose with ZSM-5 (catalyst/feed ratio = 1.5) at various temperatures.

Glucose	100 °C	200 °C	300 °C	400 °C	500 °C	600 °C	Assignment [36–38]
433	445	442	436	437	439	439	Si–O–Si external deformation (ZSM-5)
553	541	540	536	539	539	538	Si–O–Si internal deformation (ZSM-5)
	612	611	606				D6R ring mode (ZSM-5)
621							
647	641	632	699				
727	730	725					
775	775	774	779	782	781	786	Si–O sym stretch (ZSM-5)
	790	793					Si–O sym stretch (ZSM-5)
838	834	836					
914	912	912	897				
996							C–O
1023		1022					
1052		1046					
1080	1071	1068	1068	1072	1068	1072	Si–O anti-sym stretch (ZSM-5)
1111		1094					C–O
1148		1138					Ring mode (glucose)
1202	1216	1194					
1225		1217	1215	1217	1216	1216	Si–O anti-sym stretch (ZSM-5)
1295		1284					
1340	1334	1328					CH bend
1379	1363	1365	1355	1352			Sym CH bend
1460	1453	1449	1453	1457	1455		Asym. CH bend
					1492	1492	C=C
	1631	1628	1629		1625	1618	HOH bend (adsorbed water)
			1703 h	1703	1706	1706	C=O (acid carboxyl)
	1869	1866	1858	1858	1854	1858	
2890	2886	2887					CH aliphatic (glucose)
2914	2908	2910	2917	2917b	2917b	2922b	CH aliphatic
2945	2935	2941					CH aliphatic (glucose)
3356							OH (glucose)
3412							OH (glucose)

3.1.4. FTIR results

To further investigate the thermal decomposition of glucose in the presence of ZSM-5, ex situ FTIR was performed at various temperature steps. Glucose with ZSM-5 (catalyst: feed ratio = 1.5) was pyrolyzed with a heating rate of 100 °C s^{-1} to various final temperatures. Upon reaching the final reaction temperature, the probe was quenched with room temperature helium flow. FTIR was performed on the residues left in the quartz reactor. Fig. 6I shows the infrared spectra (1200–2000 cm^{-1} region) of the reaction mixture obtained at various temperatures. Fig. 6II shows the C–H stretching region (2700–4000 cm^{-1}) of the same spectra. Ramping to a final temperature of 100 or 200 °C does not alter the glucose composition significantly as the CH_2 bending modes are of similar intensity. However, it can be seen from the disappearance of the C–H bending modes of glucose at 1340, 1379 and 1460 cm^{-1} (Fig. 6I) that the glucose decomposes between 200 and 300 °C. Similarly, in Fig. 6 (II), the three aliphatic C–H modes at 2890, 2914 and 2945 cm^{-1} are lost between 200 and 300 °C.

From Fig. 6I, it can be seen that there is a new composition formed at temperatures above 400 °C from the new peaks at 1492 and 1706 cm^{-1}. At 600 °C, the presence of C=C bonds (C=C vibrations at ca. 1500 cm^{-1}) and carbonyl groups (C=O, ca. 1700 cm^{-1}) are evident. Sarbak [35] studied coke formation on HX zeolite attributes the bands at 1500 and 1589 cm^{-1} to presence of naphthalenes. Band positions for these spectra in Fig. 6 are assigned in Table 2 [36–38].

3.2. Effect of temperature on catalytic fast pyrolysis of glucose

3.2.1. Pyroprobe results

To investigate the effect of temperature on catalytic fast pyrolysis of glucose, final reaction temperatures of 400 °C, 500 °C, 600 °C, 700 °C and 800 °C were tested. A catalyst to feed ratio of 19:1 and heating rate of 1000 °C s^{-1} were used. These reaction conditions were previously determined to maximize the aromatic yield at 600 °C [6]. It can be seen in Fig. 7 that increasing reaction temperature from 400 to 800 °C increases aromatic yield up to 30% at 600 °C. At temperatures higher than 600 °C, there is little change in aromatic yield. Coke yield significantly decreases from 400 to 800 °C. The yield of carbon monoxide and carbon dioxide increase slightly over the temperature range tested. Aromatic production and coke formation vary inversely, suggesting they are competing reactions.

Fig. 8 shows the effect of temperature on the aromatic species selectivity. For simplicity, similar aromatic species are grouped together, for example, naphthalenes include the following: naphthalene, methyl-naphthalenes and ethyl-naphthalenes. As the temperature is increased from 400 to 800 °C, the selectivity to benzene increases from 10% to 30% carbon, while the selectivity for xylene and naphthalene decreases only a small amount. Changing the reaction temperature has little effect on the selectivity for toluene and the C_9 aromatics.

Table 3 summarizes the complete list of aromatics produced from catalytic fast pyrolysis of glucose in the presence of ZSM-5 at 600 °C. It can be seen that the primary aromatics produced include benzene, toluene, 1,3-dimethyl-benzene, naphthalene, 1-methyl-naphthalene and 1,5-dimethyl-naphthalene. Very large molecules such as methyl-phenanthrene are observed only in trace amounts. Naphthalenes are the largest molecules produced in significant quantities, which maybe due to the size selectivity of the zeolite catalyst. Naphthalene has a kinetic diameter of ~6.0 Å [39], which is similar to the ZSM-5 pore size of ~6.2 Å (Norman radii adjusted [40]).

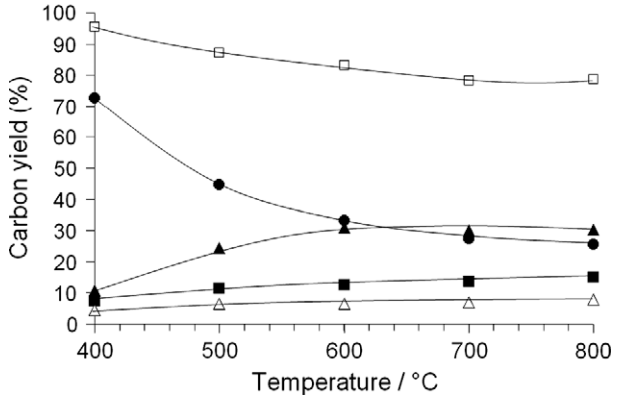

Fig. 7. Carbon yield as a function of reaction temperature for catalytic fast pyrolysis of glucose with ZSM-5. Reaction conditions: catalyst to feed weight ratio = 19; catalyst ZSM-5 (Si/Al = 15), nominal heating rate 1000 °C s^{-1}, reaction time 240 s. Key: ■: carbon monoxide, ▲: aromatics, Δ: carbon dioxide, ●: coke and □: total carbon.

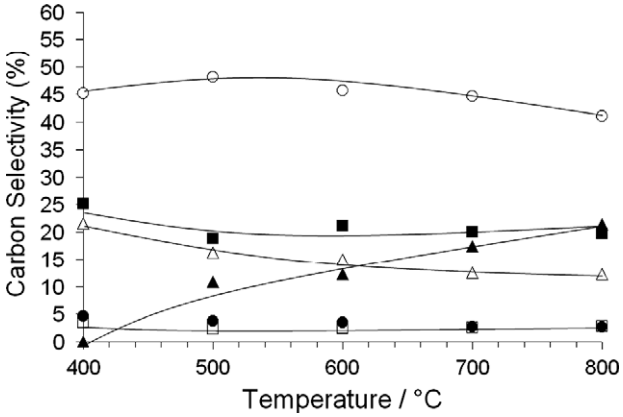

Fig. 8. Aromatic selectivity as a function of reaction temperature for catalytic fast pyrolysis of glucose with ZSM-5. Reaction conditions: catalyst to feed weight ratio = 19; catalyst ZSM-5 (Si/Al = 15), nominal heating rate 1000 °C s^{-1}, reaction time 240 s. Key: ■: toluene, ▲: benzene, Δ: xylenes and ethyl-benzene, ●: methyl-ethyl-benzene and trimethyl-benzene, □: indanes and indenes and ○: naphthalenes.

3.3. Effect of reaction time on catalytic fast pyrolysis of glucose

3.3.1. GC–MS-pyroprobe

To investigate the effect of reaction time on the yield of the catalytic fast pyrolysis products, the carbon yield of aromatics, CO and CO_2 were measured at various total reaction times from 1 and 240 s at 600 °C. Fig. 9 shows the carbon yield as a function of reaction time for the optimized reaction conditions. Initially, after 1 s of reaction, CO and CO_2 comprise the main products and increase little throughout the reaction. After 3 s reaction, the aromatic yield is higher than CO or CO_2 and increases rapidly as the reaction proceeds. After 240 s, the aromatic yield appears to be level off at a maximum carbon yield of 32%. Reaction times as little as 2 min give aromatic yields in excess of 30% carbon.

The aromatic selectivity as a function of reaction time for CFP of glucose with ZSM-5 is shown in Fig. 10. Apart from the yield of naphthalenes and indane, the selectivity of all other aromatics decreases between 1 and 3 s of reaction time at 600 °C. During this same period, the naphthalenes' selectivity dramatically increases from 18% to 40%. Naphthalenes are the major products between

Table 3
Carbon yields of aromatics produced from catalytic fast pyrolysis of glucose with ZSM-5. Reaction conditions: catalyst to feed weight ratio = 19; catalyst ZSM-5 (Si/Al = 15), nominal heating rate 1000 °C s^{-1}, reaction temperature 600 °C, reaction time 240 s.

Aromatic component	Yield (% carbon)	Selectivity (% carbon)
Benzene	4.07	12.59
Toluene	7.53	23.29
Ethylbenzene	0.18	0.57
Benzene, dimethyl-(m, o or p)	3.72	11.50
Benzene, dimethyl-(m, o or p)	1.17	3.61
Benzene, (1-methylethyl-)	0.20	0.61
Benzene, 1-ethyl-3-methyl-	0.11	0.35
1,2,4-Trimethylbenzene	0.48	1.47
Benzene, 1-ethyl-3-methyl-	0.03	0.11
Indane	0.14	0.44
Indene	0.10	0.30
Indane, 1-methyl-	0.10	0.31
1H-Indene, 1-methyl	0.07	0.22
Naphthalene	4.28	13.23
Naphthalene, 1-methyl-(m,p)	4.25	13.15
Naphthalene, 1-methyl-(m,p)	2.13	6.58
Naphthalene, 1-ethyl-	0.22	0.67
Naphthalene, 1,5-dimethyl-(m,p)	1.05	3.24
Naphthalene, 1,5-dimethyl-(m,p)	0.73	2.24
Naphthalene, 1,5-dimethyl-(m,p)	0.55	1.71
Naphthalene, 1,3-dimethyl-	0.21	0.64
Naphthalene, 1,4,6-trimethyl-	0.12	0.36
Dibenzofuran	0.06	0.18
Naphthalene, 2,3,6-trimethyl-	0.05	0.15
Naphthalene, 1,4,6-trimethyl-	0.04	0.12
Naphthalene, 1,3,6-trimethyl-	0.03	0.08
Naphthalene, 1,3,6-trimethyl-(m,p)	0.03	0.08
Fluorene	0.10	0.30
9H-fluorene, 4-methyl-	0.03	0.10
Anthracene	0.06	0.19
Phenanthrene	0.25	0.76
Anthracene, 2-methyl-	0.02	0.07
Phenanthrene, 3-methyl-	0.13	0.39
Phenanthrene, 2-methyl-	0.12	0.37

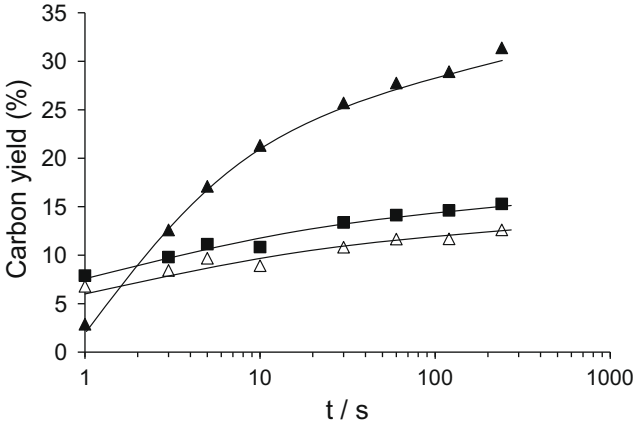

Fig. 9. Carbon yield as a function of reaction time for catalytic fast pyrolysis of glucose with ZSM-5. Reaction conditions: catalyst to feed weight ratio = 19; catalyst ZSM-5 (Si/Al = 15), nominal heating rate 1000 °C s^{-1}, reaction temperature 600 °C. Key: ■: carbon monoxide, ▲: aromatics and Δ: carbon dioxide.

3 and 240 s, and there is little selectivity change for reaction greater than 3 s.

3.3.2. FTIR results

Fig. 11 shows the infrared spectra of pure glucose after pyrolysis at 600 °C for 1 s and 120 s compared to unreacted glucose. The peak assignments are given in Table 4 [35,38]. After 1 s reaction

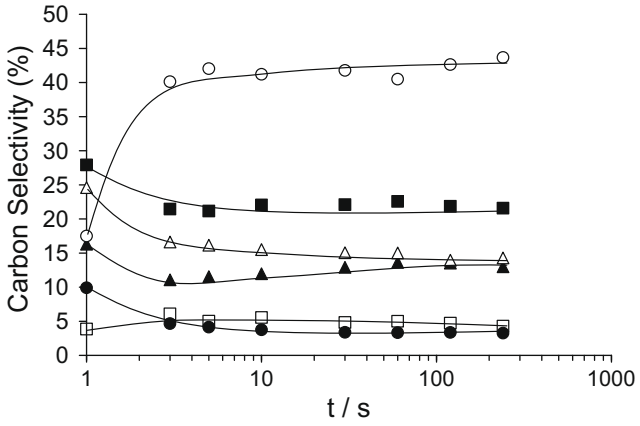

Fig. 10. Aromatic selectivity as a function of reaction time for catalytic fast pyrolysis of glucose with ZSM-5. Reaction conditions: catalyst to feed weight ratio = 19; catalyst ZSM-5 (Si/Al = 15), nominal heating rate 1000 °C s^{-1}, reaction temperature 600 °C. Key: ■: toluene, ▲: benzene, Δ: xylenes, ethyl-benzene, ●: methyl-ethyl-benzene trimethyl-benzene, □: indanes and indenes and ○: naphthalenes.

time, the CH_2 deformation modes of glucose are no longer present indicating that little unreacted glucose remains. Furthermore, the loss of the band at 1148 cm^{-1} shows that the 6-carbon ring mode is not present after 1 s reaction. The new band that appears at 1703 cm^{-1} after 1 s is characteristic of C=O stretching vibration. Therefore, the decomposition of glucose appears to go through a compound with carboxyl character [35]. For C=O stretching vibrations, 1703 cm^{-1} is in the carboxylic acid range. After even the short time of 1 s, there is very little material left in the pyroprobe reactor, only a residue film.

Fig. 12I and II shows the infrared spectra of glucose–ZSM-5 at a low catalyst to feed ratio (1.5) reacted at 600 °C for various time periods between 1 and 120 s. After 3 s reaction, the bands from the glucose (including 1460, 2890, 2914 and 2945 cm^{-1}) have completely disappeared indicating the decomposition of glucose. A longer reaction time 3 s (compared to 1 s) is required to fully decompose the glucose, which is likely due to the larger mass of glucose present. The infrared spectra of the sample after 3 s reaction at 600 °C shows two new bands at 1571 and 1711 cm^{-1} along with a broad band in the C–H stretching regions centered at 2950 cm^{-1}. The former two bands are assigned to C=C stretch and C=O stretch. The C=O stretch is in the characteristic wave number region for the diketonics present in furfuryl alcohol resins [41], while the C=C stretch may be from aromatics. A comparison of the peaks to those of furfuryl alcohol resins is given in Table 5 [36–38,41]. Therefore, the coke present after 3 s reaction has aromatic and ketone characteristics. The broad band in the C–H region indicates a broad range of organic compounds/compositions present. With further reaction time up to 120 s, these bands decrease until 120 s sample indicating these intermediates have been decomposed.

3.4. Effect of ZSM-5 to glucose ratio

3.4.1. GC–MS-pyroprobe

Previously, we have showed that high catalyst to feed ratios (>18) are required in order to maximize the aromatic yield from glucose during catalytic fast pyrolysis [5]. Fig. 13 shows the effect of catalyst to glucose ratio on the carbon yield of products at the optimal reaction conditions. Using a catalyst to feed ratio 19 produces the highest aromatic yield and lowest coke yield. The yield of partially deoxygenated species decreases from 15% to ~0% with increasing catalyst to feed ratio from 1.5 to 19. The oxygenates in-

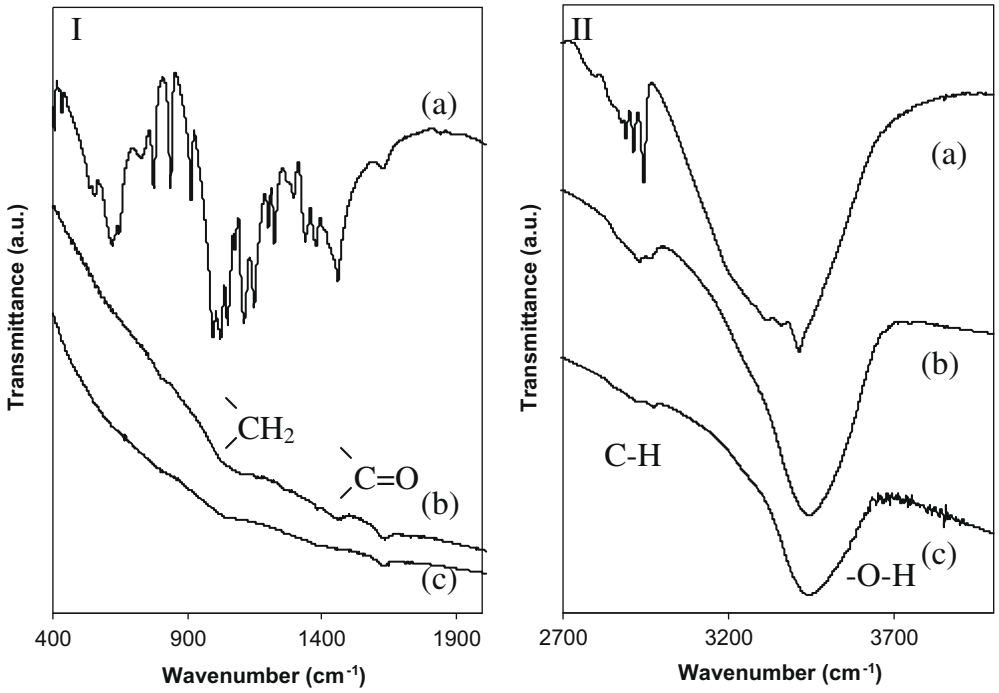

Fig. 11. FTIR spectra of pure glucose (a) unreacted and pyrolyzed at 600 °C for (b) 1 s and (c) 120 s. (I, region 400–2000 cm^{-1} and II, CH and OH stretching region 2700–4000 cm^{-1}).

Table 4
Infrared band positions (cm^{-1}) and assignments for the fast pyrolysis of glucose at 600 °C.

Glucose	1 s	120 s	Assignment [35,38]
433			Framework mode (glucose)
553			Framework mode (glucose)
621			C–C, C–O stretch (glucose)
647			C–C, C–O stretch (glucose)
727			C–C, C–O stretch (glucose)
775			CH deformation (glucose)
	797	787	CH deformation
838			CH_2CH deformation (glucose)
	873		
914			C–OH and CH deformation (glucose)
996			
1023	1021	1027	C–OH deformation (glucose)
1052			CH deformation (glucose)
1080			CH, COH deformation (glucose)
1111			CH, COH bend (glucose)
1148			Ring mode (glucose)
1202			C–O (glucose)
1225	1257		CH_2 (glucose)
1295	1374	1374	CH_2 bend, C–OH (glucose)
1340			CH bending (glucose)
1379			CH bending (glucose)
1460	1443		CH_2 bend, COH (glucose)
	1620	1621	HOH bend (adsorbed water)
	1703		C=O stretch (carboxylic)
2890	2841		CH stretch (glucose)
2914	2910	2910	CH stretch (glucose)
2945	2951	2957	CH stretch (glucose)
3356			OH stretch (glucose)
3412			OH stretch (glucose)

cludes the following: furan, 2-methyl-furan, furfural, 4-methyl-furfural, furan-2-methanol, hydroxyacetaldehyde and acetic acid. Trace amounts of anhydrosugars were also observed. The distribution of the partially deoxygenated species as a function of catalyst to glucose ratio for catalytic fast pyrolysis is shown in Fig. 14.

The aromatic selectivity is not a strong function of the catalyst to glucose ratio as shown in Fig. 15. Increasing the catalyst to feed ratio slightly increases the selectivity for toluene, xylenes and ethyl-benzene, while slightly decreasing the selectivity for benzene, methyl-ethyl-benzene, trimethyl-benzene, indanes and naphthalenes. The largest change in selectivity is for the decrease in indanes and indenes from 12% to 4% and the increase in toluene from 13% to 22%.

3.5. Conversion of oxygenated intermediates by catalytic fast pyrolysis

Using low (1.5) catalyst to feed ratio, mainly furan-based oxygenates are produced (Section 3.4.1). The partially deoxygenated species detected are likely intermediates in the formation of aromatics, since at low catalyst to feed ratios, the high quantities of oxygenates leave the reactor before they can react further to form aromatics. Using these oxygenates as feedstocks at the same reaction conditions as glucose CFP may shed light on the heterogeneous chemistry in glucose conversion to aromatics. The oxygenated intermediates; acetic acid, furan, furfural and methyl-furan were chosen as feedstocks for this study. These represent the dominant products observed at low (1.5) catalyst to feed ratios.

3.5.1. GC–MS-pyroprobe

Fig. 16 shows the products yields of catalytic pyrolysis of acetic acid, furan, furfural, methyl-furan and furfuryl alcohol. A catalyst to feed ratio of 19, 240 s reaction time and 600 °C final reaction temperature were used in this set of experiments. As shown in Fig. 16, the oxygenates form a range of aromatics, CO and CO_2. Acetic acid produces mainly CO_2 through decarboxylation, however, almost all of the remaining carbon goes to aromatics (~30% carbon yield). In the case of furan-based feedstocks, it is shown in Figs. 16 and 17 that similar yields (between 35% and 50%) and selectivity of aromatics were produced from furfural, furfuryl alcohol, furan and 2-methyl-furan. The yields of gases were also similar for the furans

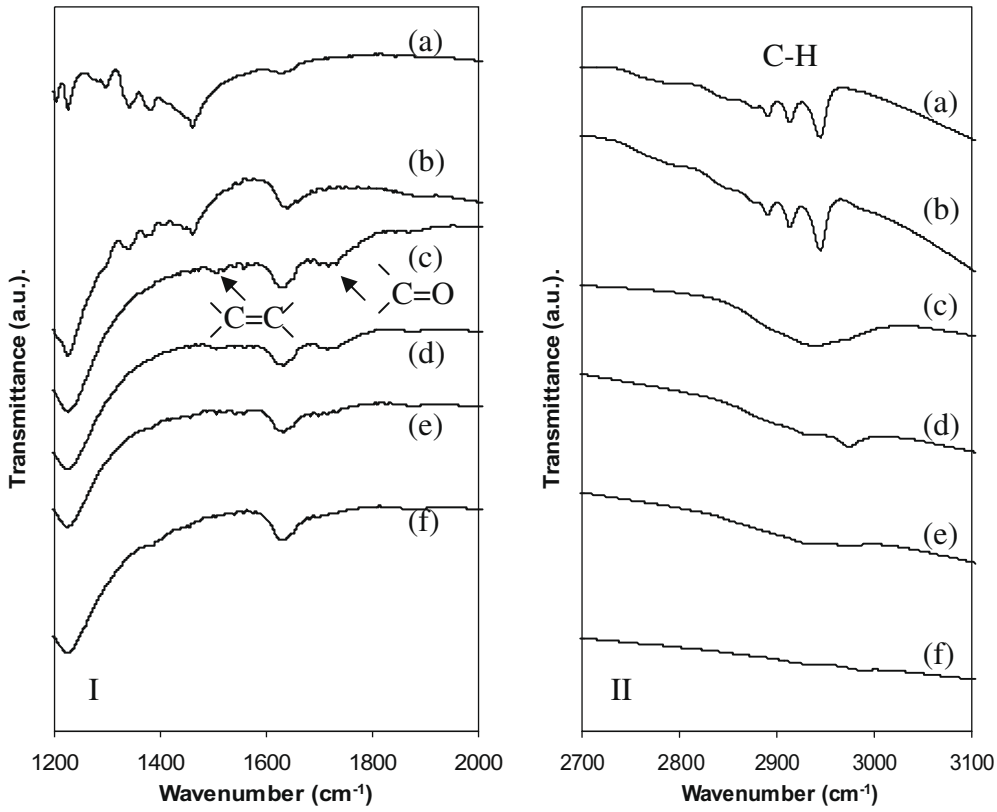

Fig. 12. Infrared spectra of (a) pure glucose and glucose with ZSM-5 (catalyst: feed ratio = 1.5) and reacted at 600 °C for various times (b) unreacted (c) 1 s, (d) 3 s, (e) 5 s and (f) 120 s. (I) 400–2000 cm^{-1} region and (II) CH stretching region (2700–3100 cm^{-1}) .

Table 5
Infrared band positions (cm^{-1}) and assignments for the fast pyrolysis of glucose with ZSM-5 (catalyst/feed ratio = 1.5) at various temperatures compared to polyfurfuryl alcohol.

Glucose	Polyfurfuryl alcohol on HY zeolite [41]	Assignment	Polyfurfuryl alcohol on HY zeolite heated to 673 K [41]	Assignment	Glucose on ZSM-5 heated to 600 °C for 1 s	Glucose on ZSM-5 heated at 600 °C for 3 s	Glucose on ZSM-5 heated at 600 °C for 120 s	Assignment [36–38]
1225					1216			Si–O anti-sym stretch (ZSM-5)
1295							1284	
1340								CH bend
1379	1375	CH bend	1350	C=C carbon			1381	Sym CH bend
1460	1422	CH bend						Asym. CH bend
	1487	Oligomeric C=C			1492			C=C
	1575	Oligomeric C=C				1571	1589	
	1628	HOH bend and carbon C=C	1630	C=C carbon	1618			HOH bend (adsorbed water)
	1710	Diketonic C=O			1706	1711		C=O (carbonyl)
	~2500				1858			
2890						2885	2912	CH (glucose)
2914	2924	C–H			2922b	2912		CH
2945						2962	2971	CH (glucose)
	3120	C–H						
3356								OH (glucose)
3412								OH (glucose)

with the exception being the increased amount of decarbonylation with the furfural feed.

3.6. Effect of coke on catalytic activity

3.6.1. GC–MS-pyroprobe

To investigate the effect of coke on the activity of ZSM-5 for the conversion of glucose, the spent catalyst was recycled and pyrolyzed again with fresh glucose. As shown in Fig. 18, the aromatic yield does not decrease with the repeated use of coked ZSM-5, indicating that the active sites of ZSM-5 remain despite the coke on the catalyst phase. In fact, the aromatic yield slightly increases with subsequent cycles. It appears that the coke deposited on the catalyst has the active form, which can be an intermediate for aromatic production. The aromatic selectivity observed for the coked catalyst after 1 and 2 times reuse is shown in Fig. 19. There is a

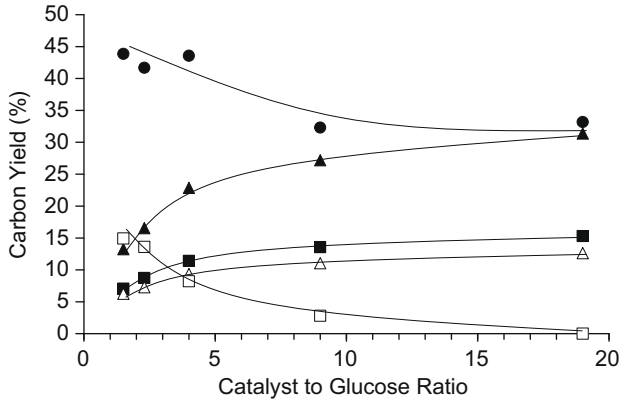

Fig. 13. Effect of catalyst to glucose ratio for catalytic fast pyrolysis. Reaction conditions: nominal heating rate 1000 °C s^{-1}, final reaction temperature 600 °C, reaction time 240 s. Carbon yield as a function of catalyst to glucose ratio. Key: ■: carbon monoxide, ▲: aromatics, Δ: carbon dioxide, □: partially deoxygenated species and ●: coke.

small decrease in the selectivity for benzene and toluene and a small increase in indanes and naphthalenes with increasing coke content. The ethyl benzenes and methyl, ethyl benzenes are unaffected by the increase in coke level.

3.6.2. N_2 adsorption of ZSM-5 before and after reaction

Coke is the major product in the conversion of glucose over ZSM-5. The yield of coke is 33% at a catalyst to feed ratio of 19 (600 °C for 240 s) and increases with decreasing catalyst concentration. To ascertain whether the coke is deposited on the outer surface of the catalyst particles and/or within the pores of ZSM-5, nitrogen adsorption was performed on ZSM-5 before reaction, after reaction at 19:1 catalyst to feed ratio and after reaction at 1.5:1 catalyst to feed ratio. Fig. 20 shows the high resolution adsorption isotherm of fresh and coked ZSM-5. The pore volumes calculated from isotherms are summarized in Table 6. It can be seen that, compared to fresh ZSM-5, the amount of adsorbed nitrogen (micropore volume) decreases from 0.12 to 0.067 cm^3g^{-1} as the coke level increases from zero to 0.7 wt.% carbon, indicating that some coke is deposited inside the zeolite pores. Further, increasing the amount of coke from 0.7 to 5 wt.% does not significantly reduce the micropore volume, which suggests further coking may take place outside of the pores on the catalyst surface.

4. Discussion

4.1. Glucose pyrolysis

Fig. 21 shows the reaction pathways that occur during catalytic fast pyrolysis of glucose. As we discovered in this study, there are two pathways for the thermal decomposition of glucose. Both pathways occur very rapidly with complete glucose decomposition in about one second at 600 °C. At low temperatures, glucose decomposes via retro-aldol and Grob fragmentation reactions to form small oxygenates such as hydroxyacetaldehyde, hydroxyacetone, dihydroxyacetone and D-glyceraldehyde. Other researchers have also shown that these small oxygenates are formed from pyrolysis of carbohydrates [25,26,42].

At high temperatures, dehydration of glucose is favored. First, glucose is dehydrated to anhydrosugars with levoglucosan as the major product. These anhydrosugars are further dehydrated to furans such as furfural, furfuryl alcohol, furan and 2-methyl-furan. Both of these decomposition pathways can occur either homogeneously or on acid sites of ZSM-5. From the FTIR results (Fig. 6), there are carboxylic acids present during decomposition, which could homogeneously catalyze dehydration. In the literature, it has been shown that furfuryl aldehyde, furfuryl alcohol and 5-hydroxymethyl furfural are prominent dehydration products from the fast pyrolysis of glucose, cellulose and hemicellulose [24,42]. In addition, Lourvanij and Rorrer [43] reported that aqueous glucose can be dehydrated with acidic zeolites to yield 5-hydroxymethylfurfural.

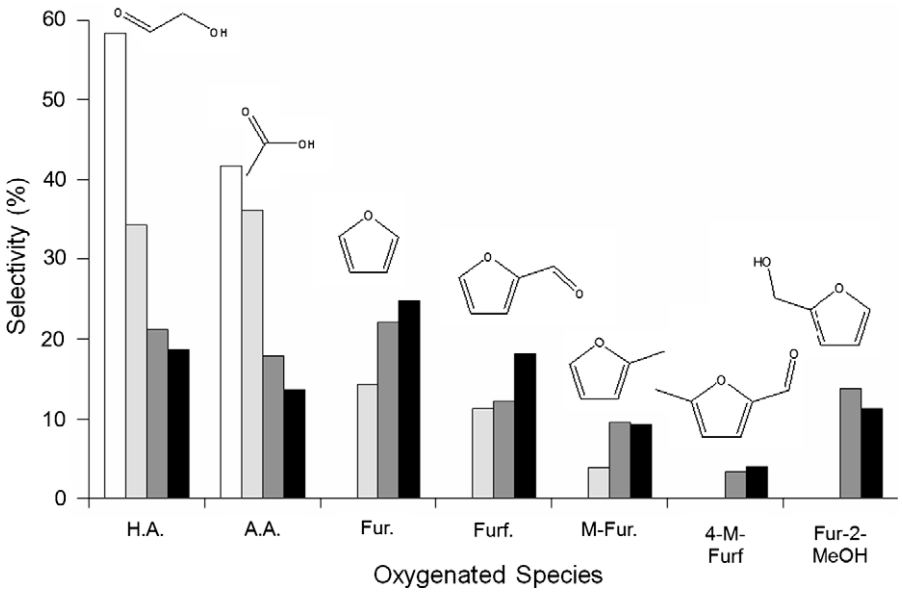

Fig. 14. Distribution of partially deoxygenated species as a function of catalyst to glucose ratio for catalytic fast pyrolysis. Reaction conditions: nominal heating rate 1000 °C s^{-1}, final reaction temperature 600 °C, reaction time 240 s. Key: catalyst:glucose ratio = 9 (white), catalyst:glucose ratio = 4 (light grey), catalyst:glucose ratio = 2.3 (dark grey), catalyst:glucose ratio = 1.5 (black). The species quantified include: (H.A.) hydroxyacetylaldehyde, (A.A.) acetic acid, (Fur.) furan, (Furf) furfural, (M-Fur) methyl furan, (4-M-Furf) 4-methylfurfural, (Fur-2-MeoH) furan-2-methanol.

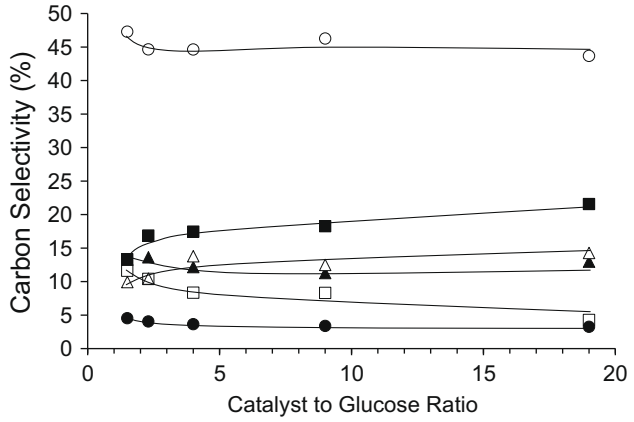

Fig. 15. Distribution of aromatic species as a function of catalyst to glucose ratio for catalytic fast pyrolysis. Reaction conditions: nominal heating rate 1000 °C s^{-1}, final reaction temperature 600 °C, reaction time 240 s. Key: ■: toluene, ▲: benzene, Δ: xylenes, ethyl-benzene, ●: methyl-ethyl-benzene trimethyl-benzene, □: indanes and indenes and ○: naphthalenes.

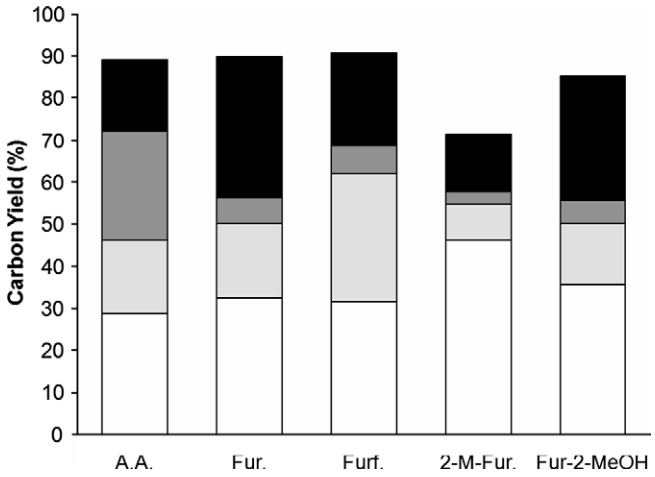

Fig. 16. Distribution of product yields as a function of intermediate compounds reacted using catalytic fast pyrolysis. Reaction conditions: nominal heating rate 1000 °C s^{-1}, final reaction temperature 600 °C, reaction time 240 s. Key: aromatics (white), carbon monoxide (light grey), carbon dioxide (dark grey), and coke (black). Abbreviations for the intermediate species are: acetic acid (A.A.), furan (Fur.), furfural (Furf.), 2-methyl furan (2-M-Fur.) and furan 2-methanol (Fur-2-MeOH).

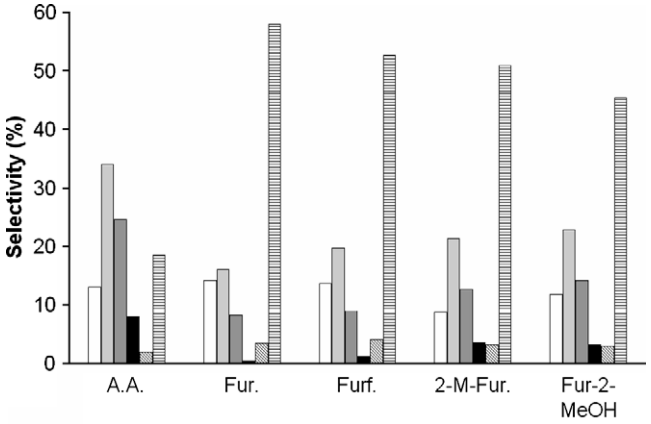

Fig. 17. Selectivity of conversion of intermediate compounds reacted using catalytic fast pyrolysis. Reaction conditions: nominal heating rate 1000 °C s^{-1}, final reaction temperature 600 °C, reaction time 240 s. Key: benzene (white), toluene (light grey), xylene and ethyl-benzene (dark grey), methyl-ethyl-benzene and trimethyl-benzene (black), indanes and indenes (diagonal lines), and Naphthalenes (horizontal lines). Abbreviations for the intermediate species are: acetic acid (A.A.), furan (Fur.), furfural (Furf.), 2-methyl furan (2-M-Fur.) and furan 2-methanol (Fur-2-MeOH).

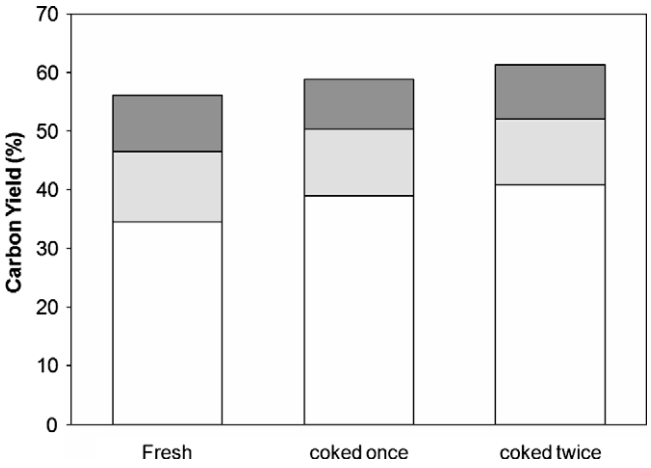

Fig. 18. Product yields in the conversion of glucose with spent catalysts at 600 °C and a catalyst to feed ratio of 19. Key: aromatics (white), carbon monoxide (light grey), and carbon dioxide (dark grey).

Williams and Besler [44] also showed that glucose has two thermal decomposition peaks between 200 and 400 °C using thermogravimetric analysis. However, these workers concluded that glucose decomposes to a polymeric intermediate, which then undergoes secondary degradation. Hence, two transitions are observed in the DTG at ~260 and 360 °C (for a heating rate of 40 °C min^{-1}). Further, Ramos-Sanchez et al. [45] reported the TGA in air of sugars including glucose. Glucose showed an onset temperature in the TGA at 192 °C with two weight losses at 227 and 321 °C.

When ZSM-5 is added to the reactor, the temperatures at which the thermal decomposition reactions occur are lowered. From the visual observations, it can be seen that coke can be formed at low temperatures (<210 °C) from the retro-aldol/Grob fragmentation products as well as at high temperatures from the dehydration products. However, coke formation is more favorable at low temperature since for pure glucose pyrolysis (Fig. 2) as well as catalytic fast pyrolysis of glucose [6] coke yield is higher at low heating rates.

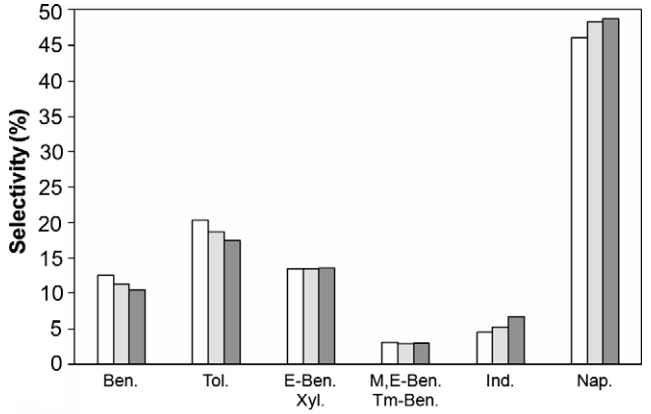

Fig. 19. Selectivity of conversion of glucose with spent catalysts at 600 °C and a catalyst to feed ratio of 19. Key: Fresh ZSM-5 (white), 1 time coked ZSM-5 (light grey), and 2 times coked ZSM-5 (dark grey).

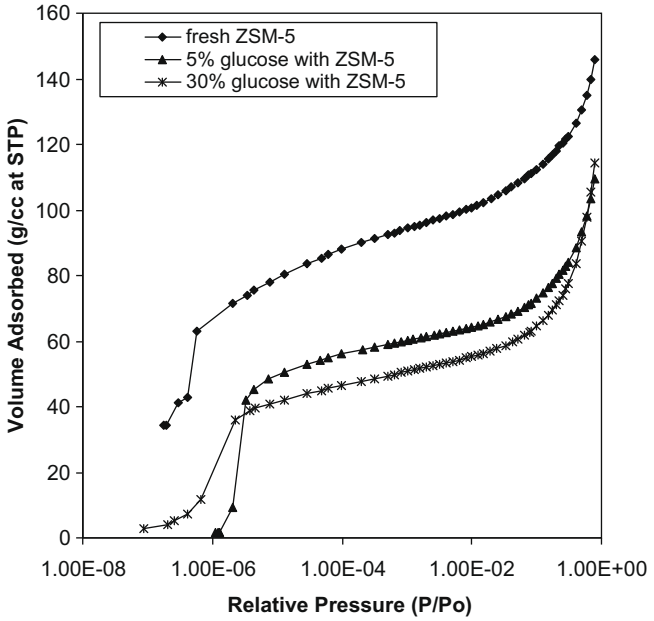

Fig. 20. High resolution adsorption isotherms (N_2 at −196 °C) of fresh ZSM-5 and coked ZSM-5 at the catalyst to feed weight ratio of 19 and 2.3.

Table 6
Micropore volume and carbon content for the fresh and coked ZSM-5.

Catalyst	Micro pore volume ($cm^3\ g^{-1}$)[a]	Carbon content (ICP analysis) (wt.%)[b]
ZSM-5 (Si/Al = 15)	0.120	–
Coked ZSM-5 (from 5 wt.% glucose at 600 °C, reacted 1×)	0.067	0.69
Coked ZSM-5 (from 30 wt.% glucose at 600 °C)	0.049	5

[a] Calculated based on the t-method.
[b] From ICP analysis. Calculation assumes organic component is primarily carbon.

4.2. Chemistry of glucose conversion to aromatics

In this study, we showed that oxygenates produced from the thermal decomposition of glucose are intermediates in the conversion of glucose to aromatics. Furan, furfural, methyl-furan and furfuryl alcohol as well as acetic acid are all converted to aromatics with similar selectivity under the same pyrolysis conditions (600 °C for 240 s). The pathway for conversion of the intermediate oxygenates to aromatics is shown in Fig. 21. From the FTIR and pyroprobe reaction time results (Figs. 9, 11 and 12), it can be seen that the formation of aromatics is the slow step in the reaction pathway. Glucose decomposes quickly in less than one second, while aromatic formation takes 2 min. To form aromatics, oxygenates diffuse into the ZSM-5 pores and through a series of decarbonylation, decarboxylation, dehydration and oligomerization reactions to form aromatics. It has been proposed that, for the conversion of methanol to aromatics with ZSM-5, the reaction proceeds through a common intermediate or "hydrocarbon pool" within the zeolite framework [33,46–48]. The methanol enters this hydrocarbon pool where it reacts with other hydrocarbons to form aromatics and olefins. The exact nature of this hydrocarbon pool has been the subject of much debate [47], but it is thought that the active species inside the hydrocarbon pool is a polymethylbenzene [33,46,48]. Recently, we have shown through isotopic labeling studies that similar hydrocarbon pool chemistry occurs during glucose conversion to aromatics over ZSM-5 [27].

The aromatic product selectivity (Fig. 10) shifts from monocyclic aromatics to naphthalenes with increasing reaction time indicating that naphthalenes are probably formed from monocyclic aromatics in second series reaction. Monocyclic aromatics from the hydrocarbon pool can either leave the reactor as products or further react with another oxygenate to form polycyclic aromatics [27].

The major competing reaction to the formation of aromatics is the formation of coke. It is likely that during CFP of glucose the intermediate furans polymerize to form resins, which further decompose to form coke on the catalyst. The acid-catalyzed dehydration polymerization of furfuryl alcohol has been well documented in the literature [41,49,50]. The FTIR reaction time data (Fig. 12, Table 5) shows at 3 s carbonyl species (band at 1711 cm^{-1}) are present. Various groups have identified 1710–1715 cm^{-1} as the characteristic band of the diketonic carbonyl present in furfuryl alcohol resins [41,49,50].

These furan resins are probably coke precursors as the band at 1711 cm^{-1} is no longer present at long reaction times. Bertarione et al. [41] reported that the furfuryl alcohol resin is decomposed on the acidic zeolite HY when heated to 400 °C to form amorphous carbon. Our FTIR results also show that unsaturated carbon is present at long reaction times (bands at 1492, 1571 and 1589 cm^{-1}).

When compared to fresh catalyst, the coked catalyst pore volume is decreased significantly; however, with increasing coke levels, there is no additional change in the pore volume. This initial decrease in pore volume is likely due to the formation of the hydrocarbon pool within the zeolite framework. Once the hydrocarbon pool is formed, additional carbon is deposited on the surface not within the pores. Several researchers studying the conversion of methanol to hydrocarbons (MTH) over ZSM-5 have reported that catalyst deactivation occurs from highly unsaturated coke on the external surface of the catalyst and not from large species within the pores [33,51,52]. In contrast, larger caged zeolites such as HY and β-zeolite are mainly deactivated by the formation of polyaromatic species within the pore systems [46,53]. The results herein suggest that the primary coking mechanism is the formation of oxygenated resins on the surface of the catalyst which ultimately decompose to unsaturated coke. However, from the results shown in Figs. 18 and 19 the level of coke on the catalyst is not sufficiently high enough to cause deactivation as the aromatic yield increases with increasing coke level. Aho et al. have shown for the pyrolysis of pine wood in the presence of ZSM-5 that further increasing the coke level on the catalyst to 16.3 wt.% leads to a significant decrease in catalytic activity [12].

4.3. Design of improved reactors for catalytic fast pyrolysis

There are several important parameters involved in maximizing the yield of aromatics from the catalytic fast pyrolysis of oxygenates over ZSM-5. High heating rates must be obtained to decrease the amount of time spent at low temperatures. At low temperatures, the primary product formed is coke. In addition, as shown in Fig. 6, moderately high reaction temperatures are required to minimize coke formation. However, the aromatic yield does not significantly increase above 600 °C, and more energy would be required for heating, hence a reaction temperature of 600 °C is the optimum. Reactor temperature can also be used to adjust the selectivity for various aromatics as shown in Fig. 7. Lastly, the concentration of oxygenates in the reactor should be low to reduce coking reactions. In addition to reducing coke, it is desirable to reduce the amount of naphthalene produced as it is of less value than the monocyclic aromatics. This can be achieved with increasing reactor temperature. Over the range from 500 to 600 °C, the selectivity to naphthalene decreases from ~50% to ~40%. Over the same temperature range, the selectivity for benzene increases from 10%

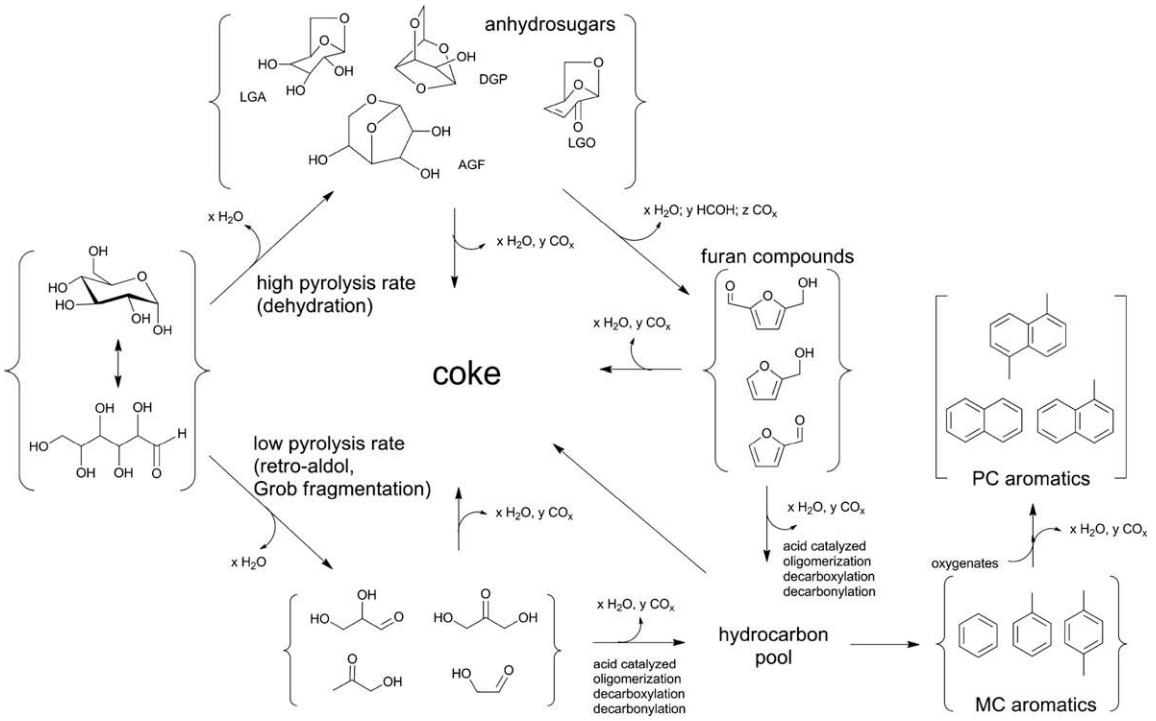

Fig. 21. Reaction chemistry for the catalytic fast pyrolysis of glucose with ZSM-5.

to 20%. Decreasing the concentration of glucose in the reactor has little effect on undesirable naphthalene formation, however, decreasing the concentration of glucose suppresses the formation of other larger aromatics such as indanes and indenes.

5. Conclusions

The catalytic fast pyrolysis of glucose involves two steps. The first step involves the rapid thermal decomposition of glucose. Glucose can decompose through two different pathways. At low temperature, glucose is decomposed to small oxygenates through retro-aldol condensation reactions. At high temperatures, glucose is dehydrated to form anhydrosugars and furans. Both decomposition pathways can occur homogeneously or on catalyst active sites. Addition of ZSM-5 to the reactor lowers the temperature at which both the decomposition reactions occur. The second step in CFP is the formation of aromatics within the pores of the zeolite. This reaction step is far slower than the preceding thermal decomposition reactions. The oxygenates produced from thermal decomposition are likely the intermediates in the formation of aromatics as furans and acetic acid produce similar aromatic products under the same pyrolysis conditions (600 °C for 240 s). The selectivity for the aromatic products is correlated to temperature and catalyst to feed ratio. The main competing reaction with aromatic production is the formation of unsaturated coke on the surface of the catalyst. Coke is formed through intermediate furan polymers, which ultimately decompose to unsaturated coke. To achieve maximum aromatic yields, pyrolysis should proceed with rapid decomposition of glucose to oxygenates to react with the catalyst. The concentration of oxygenates should remain low to avoid formation of coke and less desirable polycyclic aromatics.

Acknowledgments

The authors would like to thank the National Science Foundation-CARREER award (Grant #747996), National Science Foundation-MRI award and the National Science Council (Taiwan, Grant #096-2917-I-564-114) for the generous funding. We would also like to acknowledge Phillip R. Westmoreland for help with the pyroprobe and W. Curt Conner for technical assistance.

References

[1] L.R. Lynd, C.E. Wyman, T.U. Gerngross, Biotechnology Progress 15 (1999) 777–793.
[2] C.E. Wyman, Annual Review of Energy and the Environment 24 (1999) 189.
[3] C.E. Wyman, B.E. Dale, R.T. Elander, M. Holtzapple, M.R. Ladisch, Y.Y. Lee, Bioresource Technology 96 (2005) 1959–1966.
[4] D.L. Klass, Biomass for Renewable Energy, Fuels, and Chemicals, Academic Press, San Diego, 1998.
[5] T.R. Carlson, G.A. Tompsett, W.C. Conner, G.W. Huber, Topics in Catalysis 52 (2009) 241–252.
[6] T.R. Carlson, T.R. Vispute, G.W. Huber, ChemSusChem 1 (2008) 397–400.
[7] A.A. Lappas, M.C. Samolada, D.K. Iatridis, S.S. Voutetakis, I.A. Vasalos, Fuel 81 (2002) 2087–2095.
[8] M. Olazar, R. Aguado, J. Bilbao, A. Barona, AIChE Journal 46 (2000) 1025–1033.
[9] J. Adam, E. Antonakou, A. Lappas, M. Stoecker, M.H. Nilsen, A. Bouzga, J.E. Hustad, G. Oye, Microporous and Mesoporous Materials 96 (2006) 93–101.
[10] D. Fabbri, C. Torri, V. Baravelli, Journal of Analytical and Applied Pyrolysis 80 (2007) 24–29.
[11] A. Pattiya, J.O. Titiloye, A.V. Bridgwater, Journal of Analytical and Applied Pyrolysis 81 (2008) 72–79.
[12] A. Aho, N. Kumar, K. Eraenen, T. Salmi, M. Hupa, D.Y. Murzin, Fuel 87 (2008) 2493–2501.
[13] H.B. Goyal, D. Seal, R.C. Saxena, Renewable & Sustainable Energy Reviews 12 (2007) 504–517.
[14] A. Demirbas, Energy Sources, Part A: Recovery, Utilization, and Environmental Effects 29 (2007) 753–760.
[15] N.Y. Chen, T.F. Degnan Jr., L.R. Koenig, Chemtech 16 (1986) 506–511.
[16] M.I. Hanniff, L.H. Dao, Energy from Biomass and Wastes 10 (1987) 831–843.
[17] M.I. Hanniff, L.H. Dao, Applied Catalysis 39 (1988) 33–47.
[18] M.C. Samolada, W. Baldauf, I.A. Vasalos, Fuel 77 (1998) 1667–1675.
[19] J.D. Adjaye, N.N. Bakhshi, Fuel Processing Technology 45 (1995) 161–183.
[20] R.K. Sharma, N.N. Bakhshi, Canadian Journal of Chemical Engineering 71 (1993) 383–391.
[21] A.V. Bridgwater, M.L. Cottam, Energy & Fuels 6 (1992) 113–120.
[22] P.A. Horne, P.T. Williams, Fuel 75 (1996) 1043–1050.
[23] L.H. Dao, M. Haniff, A. Houle, D. Lamothe, Preprints of Papers – American Chemical Society, Division of Fuel Chemistry 32 (1987) 308–316.
[24] J.B. Paine, Y.B. Pithawalla, J.D. Naworal, Journal of Analytical and Applied Pyrolysis 83 (2008) 37–63.

[25] J.B. Paine, Y.B. Pithawalla, J.D. Naworal, Journal of Analytical and Applied Pyrolysis 82 (2008) 10–41.
[26] J.B. Paine, Y.B. Pithawalla, J.D. Naworal, Journal of Analytical and Applied Pyrolysis 82 (2008) 42–69.
[27] T.R. Carlson, J. Jae, G.W. Huber, ChemCatChem 1 (2009) 107–110.
[28] D. Mohan, C.U. Pittman Jr., P.H. Steele, Energy & Fuels 20 (2006) 848–889.
[29] J. Lede, F. Blanchard, O. Boutin, Fuel 81 (2002) 1269–1279.
[30] Y.-C. Lin, J. Cho, G.A. Tompsett, P.R. Westmoreland, G.W. Huber, Journal of Physical Chemistry C 113 (2009) 20097–20107.
[31] K. Bilba, A. Ouensanga, Journal of Analytical and Applied Pyrolysis 38 (1996) 61–73.
[32] R.K. Sharma, J.B. Wooten, V.L. Baliga, M.R. Hajaligol, Fuel 80 (2001) 1825–1836.
[33] M. Bjorgen, S. Svelle, F. Joensen, J. Nerlov, S. Kolboe, F. Bonino, L. Palumbo, S. Bordiga, U. Olsbye, Journal of Catalysis 249 (2007) 195–207.
[34] D.R. Lide, CRC Handbook of Chemistry and Physics: A Ready-Reference Book of Chemical and Physical Data, CRC Press, Boca Raton, Fla, 2008.
[35] Z. Sarbak, Reaction Kinetics and Catalysis Letters 69 (2000) 177–181.
[36] A. Miecznikowski, J. Hanuza, Zeolites 7 (1987) 249–254.
[37] P. Walther, Zeitschrift fuer Physikalische Chemie (Leipzig) 269 (1988) 809–812.
[38] H.A. Wells Jr., R.H. Atalla, Journal of Molecular Structure 224 (1990) 385–424.
[39] D.M. Ruthven, B.K. Kaul, Industrial and Engineering Chemistry Research 32 (1993) 2053–2057.
[40] M. Cook, W.C. Conner, in: Proceedings of the International Zeolite Conference, 12th, Baltimore, July 5–10, 1998, vol. 1, 1999, pp. 409–414.
[41] S. Bertarione, F. Bonino, F. Cesano, A. Damin, D. Scarano, A. Zecchina, Journal of Physical Chemistry B 112 (2008) 2580–2589.
[42] R.J. Evans, T.A. Milne, Energy & Fuels 1 (1987) 123–137.
[43] K. Lourvanij, G.L. Rorrer, Journal of Chemical Technology & Biotechnology 69 (1997) 35–44.
[44] P.T. Williams, S. Besler, Advances in Thermochemical Biomass Conversion 2 (1994) 771–783.
[45] M.C. Ramos-Sanchez, F.J. Rey, M.L. Rodriguez, F.J. Martin-Gil, J. Martin-Gil, Thermochimica Acta 134 (1988) 55–60.
[46] J.F. Haw, W.G. Song, D.M. Marcus, J.B. Nicholas, Accounts of Chemical Research 36 (2003) 317–326.
[47] M. Stocker, Microporous and Mesoporous Materials 29 (1999) 3–48.
[48] D.M. McCann, D. Lesthaeghe, P.W. Kletnieks, D.R. Guenther, M.J. Hayman, V. Van Speybroeck, M. Waroquier, J.F. Haw, Angewandte Chemie – International Edition 47 (2008) 5179–5182.
[49] M. Choura, N.M. Belgacem, A. Gandini, Macromolecules 29 (1996) 3839.
[50] R.T. Conley, I. Metil, Journal of Applied Polymer Science 7 (1963) 37.
[51] D. Mores, E. Stavitski, M.H.F. Kox, J. Kornatowski, U. Olsbye, B.M. Weckhuysen, Chemistry – A European Journal 14 (2008) 11320–11327.
[52] N.K. Bar, F. Bauer, D.M. Ruthven, B.J. Balcom, Journal of Catalysis 208 (2002) 224–228.
[53] M. Bjorgen, U. Olsbye, S. Kolboe, Journal of Catalysis 215 (2003) 30–44.